AIP | Applied Physics Letters

Effect of dynamical Coulomb interaction on junctionless transistor performance: Monte Carlo study of plasmon excitations

Katsuhisa Yoshida, Toru Shibamiya, and Nobuyuki Sano

Citation: Applied Physics Letters **105**, 033501 (2014); doi: 10.1063/1.4890695
View online: http://dx.doi.org/10.1063/1.4890695
View Table of Contents: http://scitation.aip.org/content/aip/journal/apl/105/3?ver=pdfcov
Published by the AIP Publishing

Effect of dynamical Coulomb interaction on junctionless transistor performance: Monte Carlo study of plasmon excitations

Katsuhisa Yoshida,[a] Toru Shibamiya, and Nobuyuki Sano
Institute of Applied Physics, University of Tsukuba, 1-1-1 Tennodai, Tsukuba, Ibaraki 305-8573, Japan

(Received 19 February 2014; accepted 9 July 2014; published online 21 July 2014)

We study the dynamical Coulomb interaction under the junctionless transistor (JLT) structures, in which high doping concentration is inevitable to obtain good device performance, by employing the self-consistent Monte Carlo simulations. The power spectra of potential fluctuations in the source and drain regions show clear peaks corresponding to the plasma frequencies in those regions. This observation justifies the accuracy of the present simulations. The dynamical Coulomb interaction degrades the drain current and, thus, is inevitable to predict accurate device performance of JLTs. © *2014 AIP Publishing LLC*. [http://dx.doi.org/10.1063/1.4890695]

The conventional scaling of Si metal-oxide-semiconductor field-effect transistors (MOSFETs) is about to approach its fundamental limits imposed by physics intrinsic in transport phenomena, and various alternative device structures have been proposed. Among them is the junctionless transistor (JLT),[1,2] which has recently received considerable attention. Main advantage of JLTs lies in the fact that there is no need to fabricate abrupt junction between source/drain and channel. In addition, electrons flow in the channel far from the gate-insulator interface, and, thus, surface roughness scattering which is the dominant scattering center to degrade device performance in inversion-type FETs, could be minimized. However, the device parameters such as cross-section, channel length, substrate doping concentration, etc., have to be carefully optimized to gain sharp subthreshold and good current-voltage (I-V) characteristics.[3–7] Therefore, many numerical and theoretical analyses[8–12] have been carried out to clarify such criteria.

However, relatively less attention has been paid on the fact that the device substrate has to be highly doped, namely $10^{19}\,cm^{-3}$ or above, to gain large drain current in on-condition. The impurity scattering and the long-range and short-range electron-electron interactions begin to dominate electron transport under such highly doped regimes, even though the doping concentration is smaller than the densities in source and drain regions of the conventional FETs. Moreover, one may consider that quantum confined effects become more important in smaller body devices which are demanded in highly doped JLTs and the quantum corrections largely impact on subthreshold characteristics. Even though the thickness becomes thinner and the confined effects becomes more significant, the Coulomb interaction is unavoidable problems in such high doped structures.

As a result, the Coulomb interaction among electrons and impurities may strongly affect the device performance. In the present Letter, we study the static and dynamical Coulomb interaction under the JLT structures by employing the self-consistent Monte Carlo (MC) simulations, with which the Coulomb interaction has been accurately taken into account in the past analysis for inversion-type double-gate FETs.[13,14] Note that the MC simulation cannot predict reliable subthreshold characteristics due to statistical uncertainty caused by too small number of carriers. Thus, we study the Coulomb interaction especially for the characteristics of the drain current versus drain voltage.

The MC method employed in the present study is self-consistently coupled with the three-dimensional Poisson equation and includes all relevant scattering processes such as acoustic and optical phonon scattering, ionized impurity scattering, and the short-range electron–electron scattering under the frame work of the nonparabolic band structure of Si. Spatial grid and time step to update the long-range electrostatic potential are chosen to be fine enough to resolve the dynamical potential modulation (collective excitation of plasma waves), as well as to reproduce the correct electron mobility under high-impurity concentrations.[15,16] Figure 1 shows the device structure introduced into our MC simulations, i.e., the JLT with the cross section of $10 \times 10\,nm^2$ surrounded by the metallic gate with 50 nm long. The donor concentration of Si substrate is assumed to be $10^{19}\,cm^{-3}$, and the thickness of gate insulator (SiO_2) is 0.86 nm. We should comment on the gate voltage condition employed in the present study. Although the biasing condition required from the circuit applications is indeed essential, we consider the biasing condition here such that the device characteristics are controlled mainly by the channel transport. In the conventional FETs, the potential profile and scattering processes in channel region determines the device performance because the channel shows the highest "resistance" in the structure. In JLTs, however, the gate voltage can change this scenario

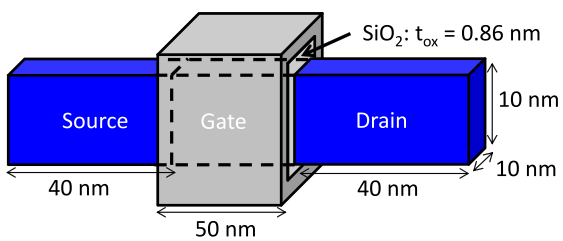

FIG. 1. Schematic drawing of Si nanowire JLT structure employed in the present MC simulations. The donor concentration in the substrate, assumed to be fully ionized, is $10^{19}\,cm^{-3}$. t_{ox} is the oxide thickness.

[a]Electronic mail: yoshida@hermes.esys.tsukuba.ac.jp

in the following manners. Under the gate voltage of $V_G = V_{FB}$ where V_{FB} is the flat-band voltage, there is no potential difference between the source and channel regions. Thus, carrier density becomes uniform in the substrate, and parasitic resistances in the source, channel, and drain regions become the same. In this regime, device characteristics are not only described by the channel properties but also by the conditions of source and drain regions. Therefore, on the contrary to the regular inversion-mode FETs, we select the gate voltage regime in smaller than the flat-band voltage.

The electrostatic potential profile, which is time-averaged over 20 ps, is shown in Fig. 2(a) in the channel direction from the source to drain under the drain voltage of $V_D = 0.6\,\mathrm{V}$ and the gate voltage of $V_G = V_{FB} - 0.3\,\mathrm{V}$. The potential is evaluated in the middle plane of the cross-section of nanowire. The electron density along the channel direction in the same bias condition is plotted in Fig. 2(b). Notice that the electrostatic potential temporally fluctuates associated with the plasma oscillations, yet time-averaged potential is rather smooth. This claims and justifies the stability of the present MC simulations. Also, the electron density is large in the middle of the channel of nanowire, and becomes smaller near the drain, which plays a role of pinch-off in conventional FETs.

The spatially averaged power spectra of potential fluctuations in the source and drain regions are presented in Figs. 3(a) and 3(b), respectively. The bias condition is the same as that in Fig. 2. The arrows in the figures indicate the plasma frequencies for two different electron densities (2×10^{18} and $10^{19}\,\mathrm{cm}^{-3}$). Since the time range with which phonon scattering takes place is close to the inverse of the plasma frequencies, the power spectra are broadened due to the finiteness of the lifetime of plasmons. Nevertheless, we observe a clear peak in the source region around the plasma frequency corresponding to the electron density of $10^{19}\,\mathrm{cm}^{-3}$ and the collective excitation (plasmon) is properly simulated in the present MC simulations. On the other hand, a few broad peaks corresponding to the electron densities from 2×10^{18} to $10^{19}\,\mathrm{cm}^{-3}$ are seen in the drain region. The inset to Fig. 3(b) shows the power spectra in the two regions, namely, near the channel region and the contact region inside the drain. Since the electron density in the drain is greatly lowered ($\sim 10^{18}\,\mathrm{cm}^{-3}$) near the channel region at high drain voltage, as clearly shown in Fig. 2(b), it is reasonable to expect that the first peak in the spectra corresponds to the plasmon excitation in that region due to the injection of high energy channel electrons into the drain accelerated by the potential drop near the drain. As one moves intro the drain, the electron density approaches the quasi-equilibrium value ($10^{19}\,\mathrm{cm}^{-3}$) in the drain, and, thus, the power spectrum becomes a double-peak structure and spreads over wide frequency regions.

The consequence of dynamical Coulomb interaction on I-V characteristics is presented in Fig. 4 where the drain current versus drain voltage characteristics obtained from two

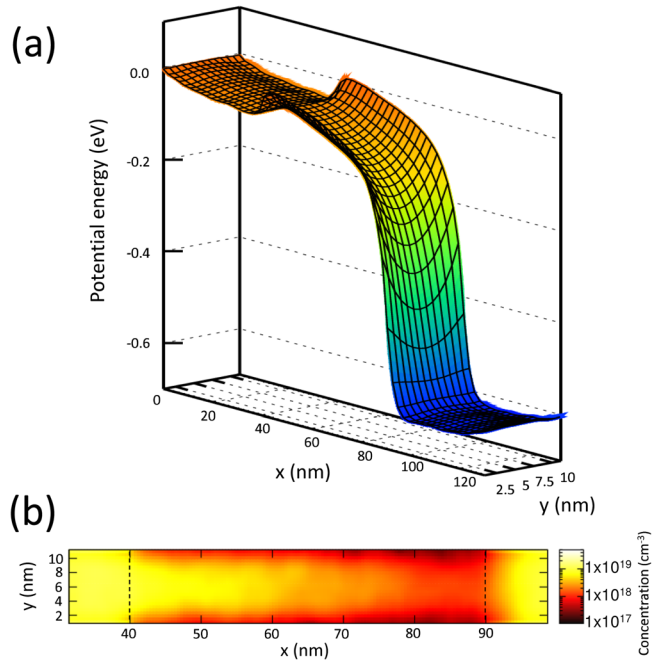

FIG. 2. (a) Time averaged potential profile in middle plane under the bias condition of gate voltage of $V_G - V_{FB} = -0.3\,\mathrm{V}$ and drain voltage of $V_D = 0.6\,\mathrm{V}$. The x and y axes are, respectively, the direction from the source to the drain region and the width direction of nanowire. (b) Electron concentration in the same plane in (a).

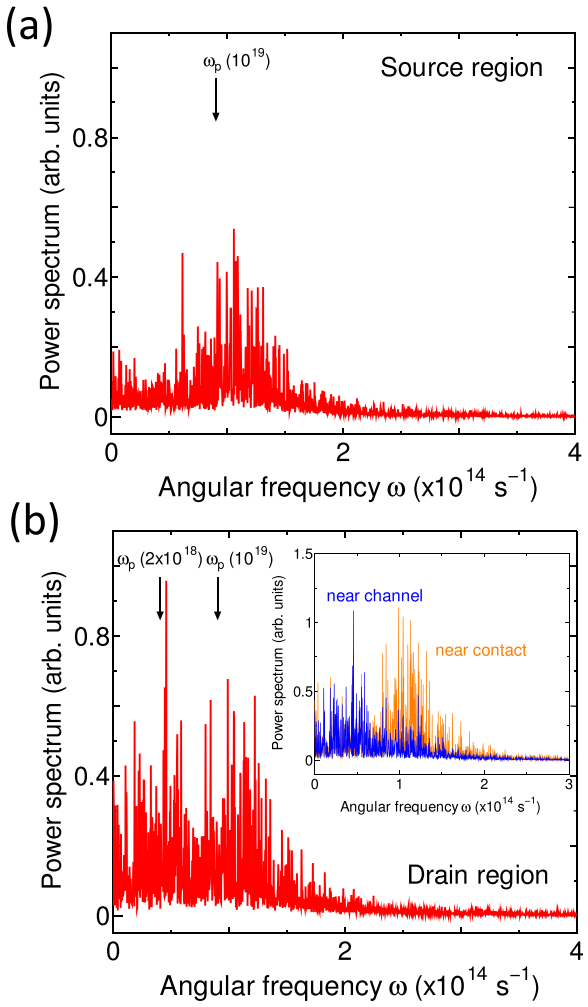

FIG. 3. Spatially averaged power spectra of potential fluctuations under the bias condition of gate voltage of $V_G - V_{FB} = -0.3\,\mathrm{V}$ and drain voltage of $V_D = 0.6\,\mathrm{V}$ in (a) source and (b) drain regions. Inset figure in (b): Spatially averaged power spectra in the drain region near the channel and the contact. $\omega_p(2 \times 10^{18})$ and $\omega_p(10^{19})$ are the plasma frequencies of electron concentrations of 10^{18} and $10^{19}\,\mathrm{cm}^{-3}$.

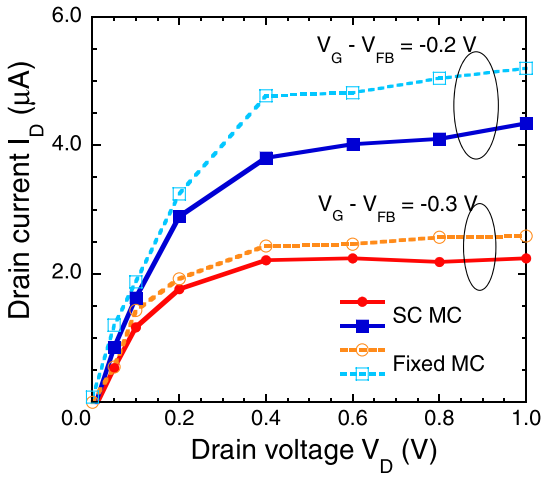

FIG. 4. Drain current I_D versus drain voltage V_D characteristics at gate voltage $V_G - V_{FB} = -0.3$ and -0.2 V. The results show the self-consistent MC simulations coupled with the Poisson equation are denoted as "SC MC", whereras "Fixed MC" represents those from the MC simulation under the time averaged potential.

different MC simulations are shown: The results from the MC simulations under the fixed potential, in which the dynamical long-range potential fluctuations are switched off, are also plotted along with the self-consistent MC simulations. The fixed potential is obtained by averaging the potentials of the self-consistent MC simulations over long time period. The self-consistent MC simulation predicts lower drain current, though its magnitude is not large in each gate voltage condition. This tendency is consistent with those found previously for the inversion-type FETs:[14,16] The dynamical screening taken place near the drain/source associated with the long-range Coulomb interaction between the channel electrons and electrons in the drain/source degrades drain current. A similar scenario holds true in the present case and the details of current degradation will be discussed elsewhere.

We would like to stress that although the difference in current between two MC simulations is not large, this does not imply that the dynamical Coulomb interaction is insignificant. The averaged potential employed here is obtained from the self-consistent MC simulations and, thus, very close to the "correct" averaged potential. In other words, the correct I-V characteristics cannot be obtained without taking into account the dynamical Coulomb interaction in any device simulations.

In summary, we have studied the dynamical Coulomb interaction in JLT by self-consistent MC simulations. The dynamical effects in source and drain regions would be smaller than those of conventional FETs because the plasma frequency in the present study ω_p electron density $\sim 10^{19}$ cm^{-3} is smaller than the frequency of the conventional FET ω_p electron density $\sim 10^{20}$ cm^{-3}. However, due to high doping concentration in the substrate, the dynamical Coulomb interaction is inevitable. The collective mode (plasmon) excitation associated with the temporal long-range Coulomb interaction has been simulated in the source and drain regions. Consequently, the dynamical Coulomb interaction degrades drain current, compared with that in MC simulations under the averaged electrostatic potential. This difference is expected to be much larger, unless the "correct" averaged potential is available, and, thus, including the dynamical Coulomb interaction is inevitable to predict accurate device pefromance of JLTs.

This work was supported in part by Ministry of Education, Science, Sports, and Culture under Grant-in-Aid for Scientific Research (B) (No. 24360130).

[1]C. Lee, A. Afzalian, N. D. Akhavan, R. Yan, I. Ferain, and J. Colinge, Appl. Phys. Lett. **94**, 053511 (2009).
[2]J. Colinge, C. Lee, A. Afzalian, N. Akhavan, R. Yan, I. Ferain, P. Razavi, O. Brendan, A. Blake, M. White, A. Kelleher, M. Brendan, and R. Murphy, Nat. Nanotechnol. **5**, 225 (2010).
[3]C. Lee, A. Borne, I. Ferain, A. Afzalian, R. Yan, N. D. Akhavan, P. Razavi, and J. Colinge, IEEE Trans. Electron Devices **57**, 620 (2010).
[4]S. Choi, D. Moon, S. Kim, J. P. Duarte, and Y. Choi, IEEE Electron Device Lett. **32**, 125 (2011).
[5]S. Barraud, M. Berthomé, R. Coquand, M. Casse, T. Ernst, M. Samson, P. Perreau, K. K. Bourdelle, O. Faynot, and T. Poiroux, IEEE Electron Device Lett. **33**, 1225 (2012).
[6]D. Moon, S. Choi, J. P. Duarte, and Y. Choi, IEEE Trans. Electron Devices **60**, 1355 (2013).
[7]D. Jeon, S. Park, M. Mouis, M. Berthomé, S. Barraud, G. Kim, and G. Ghibaudo, Solid-State Electron. **90**, 86 (2013).
[8]C. Lee, I. Ferain, A. Afzalian, R. Yan, N. D. Akhavan, P. Razavi, and J. Colinge, Solid-State Electron. **54**, 97 (2010).
[9]J. Colinge, A. Kranti, R. Yan, C. Lee, I. Ferain, R. Yu, N. D. Akhavan, and P. Razavi, Solid-State Electron. **65–66**, 33 (2011).
[10]J. P. Duarte, S. Choi, D. Moon, and Y. Choi, IEEE Electron Device Lett. **32**, 704 (2011).
[11]S. Gundapaneni, M. Bajaj, R. K. Pandey, K. V. R. M. Murali, S. Ganguly, and A. Kottantharayil, IEEE Trans. Electron Dev. **59**, 1023 (2012).
[12]F. Jazaeri, L. Barbut, A. Koukab, and J. Sallese, Solid-State Electron. **82**, 103 (2013).
[13]M. V. Fischetti and S. E. Laux, J. Appl. Phys. **89**, 1205 (2001).
[14]K. Nakanishi, T. Uechi, and N. Sano, in *Self-Consistent Monte Carlo Device Simulations Under Nano-Scale Device Structures: Role of Coulomb Interaction, Degeneracy, and Boundary Condition Baltimore, MD, 7–9 December 2009* (IEEE, 2009), pp. 1–4.
[15]T. Fukui, T. Uechi, and N. Sano, Appl. Phys. Express **1**, 051407 (2008).
[16]N. Sano, Jpn. J. Appl. Phys., Part 1 **50**, 010108 (2011).